

V. Experimental studies of QCD

1. Test of QCD in e^+e^- annihilation
2. Structure of the proton
3. Structure functions and quark densities
4. Scaling violation in DIS

1. Test of QCD in e^+e^- annihilation

1.1 Two-jet events and production of colored $q \bar{q}$

a) clear two-jet event structure in $e^+e^- \rightarrow \text{hadrons} (q\bar{q})$

b) $R_{had} = \frac{\sigma(ee \rightarrow \text{hadrons})}{\sigma(ee \rightarrow \mu\mu)}$ indicates fractional charges and $N_c=3$

Additional indications for $N_c=3$:

- Δ^{++} statistic problem:

Spin $J(\Delta^{++})=3/2$ ($L=0$), quark content $|uuu\rangle$

$\rightarrow |\Delta^{++}\rangle = |u\uparrow u\uparrow u\uparrow\rangle$ forbidden by Fermi statistic

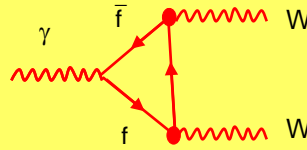
Solution is additional quantum number for quarks (color)

$$|\Delta^{++}\rangle = \frac{1}{\sqrt{6}} \varepsilon_{ijk} |u_i\uparrow u_j\uparrow u_k\uparrow\rangle \quad i, j, k = \text{color index}$$

Additional indications for $N_C=3$:

- Triangle anomalie

Divergent fermion loops



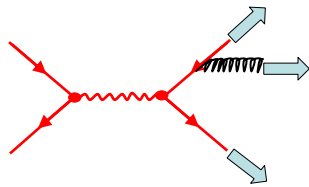
Divergences cancel if $N_C = 3$:

$$0 = \sum_f Q_f = (-1) + (-1) + (-1) + N_C \cdot \left[\left(\frac{2}{3} - \frac{1}{3} \right) \cdot 3 \right]$$

3 generations of u/d-type quark

1.2 Discovery of the gluon

Discovery of 3-jet events by the TASSO collaboration (PETRA) in 1977:



3-jet events are interpreted as quark pairs with an additional hard gluon.

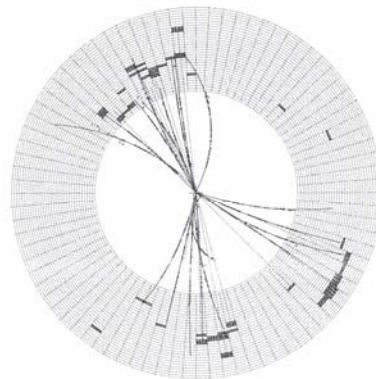


Fig. 11.12 A three-jet event observed by the JADE detector at PETRA.

$$\frac{\#3\text{-jet events}}{\#2\text{-jet events}} \approx 0.15 \sim \alpha_s$$

at $\sqrt{s}=20\text{ GeV}$



α_s is large

Spin of the gluon

Ellis-Karlinger angle

Ordering of 3 jets: $E_1 > E_2 > E_3$

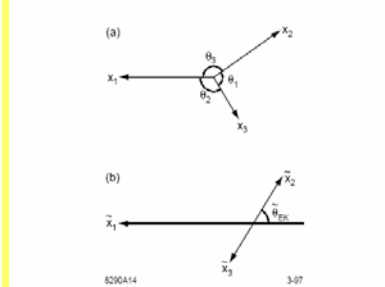


Figure 8: (a) Representation of the momentum vectors in a three-jet event, as (b) definition of the Ellis-Karlinger angle.

Measure direction of jet-1 in the rest frame of jet-2 and jet-3: θ_{EK}

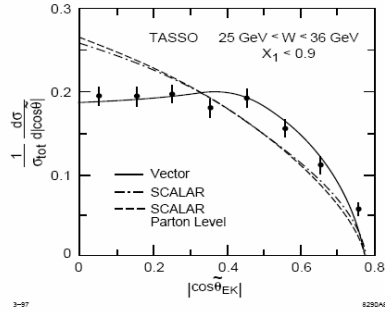
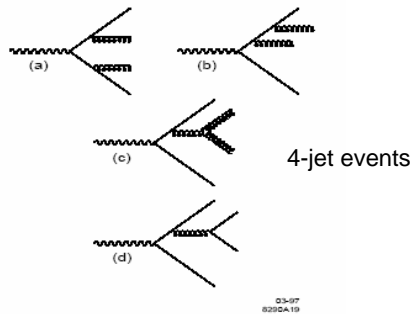


Figure 9: The Ellis-Karlinger angle distribution of three-jet events recorded by TASSO at $Q \sim 30$ GeV [18]; the data favour spin-1 (vector) gluons.

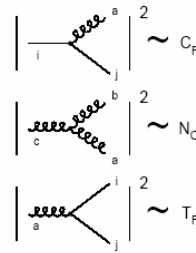
Gluon spin $J=1$

1.3 Multi-jet events and gluon self coupling

Non Abelian gauge theory (QCD)



Casimir (color) factors:



4-jet cross section:

$$\frac{1}{\sigma_0} d\sigma^4 = \left(\frac{\alpha_s C_F}{\pi}\right)^2 \left[F_A + \left(1 - \frac{1}{2} \frac{N_C}{C_F}\right) F_B + \frac{N_C}{C_F} F_C \right] + \left(\frac{\alpha_s C_F}{\pi}\right)^2 \left[\frac{T_F}{C_F} N_f F_D + \left(1 - \frac{1}{2} \frac{N_C}{C_F}\right) F_E \right]$$

$F_{A,B,C,D,E}$ are kinematic functions

Group	N_C	C_F	T_F
U(1)	0	1	1
U(1) ₃	0	1	3
SU(N)	N	$(N^2 - 1)/2N$	1/2
SU(3)	3	4/3	1/2

Exploiting the angular distribution of 4-jets:

- Bengtson-Zerwas angle

$$\cos \chi_{BZ} \propto (\vec{p}_1 \times \vec{p}_2) \cdot (\vec{p}_3 \times \vec{p}_4)$$

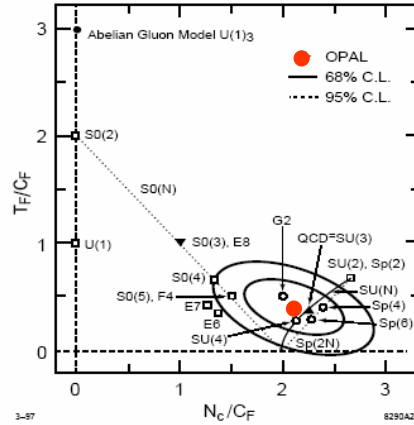
- Nachtmann-Reiter angle

$$\cos \theta_{NR} \propto (\vec{p}_1 - \vec{p}_2) \cdot (\vec{p}_3 - \vec{p}_4)$$

Allows to measure the ratios T_F/C_F and N_C/C_F

SU(3) predicts: $T_F/C_F = 0.375$ and $N_C/C_F = 2.25$

$N_C/C_F \neq 0 \rightarrow$ contribution from gluon self-coupling in the 4-jet events



Confirms QCD prediction (SU(3)) and gluon self-coupling

1.4 Measurement of strong coupling α_s

\rightarrow α_s measurements are done at fixed scale Q^2 : $\alpha_s(Q^2)$

a) α_s from total hadronic cross section

$$\sigma_{had}(s) = \sigma_{had}^{QED}(s) \left[1 + \frac{\alpha_s(s)}{\pi} + 1.411 \cdot \frac{\alpha_s(s)^2}{\pi^2} + \dots \right]$$

$$R_{had} = \frac{\sigma(ee \rightarrow hadrons)}{\sigma(ee \rightarrow \mu\mu)} = 3 \sum Q_q^2 \left\{ 1 + \frac{\alpha_s}{\pi} + 1.411 \frac{\alpha_s^2}{\pi^2} + \dots \right\}$$

Not very precise.

$\rightarrow \alpha_s(s)$

b) α_s from hadronic event shape variables

3-jet rate: $R_3 \equiv \frac{\sigma_{3-jet}}{\sigma_{had}}$ depends on α_s

3-jet rate is measured as function of a jet resolution parameter y_{cut}

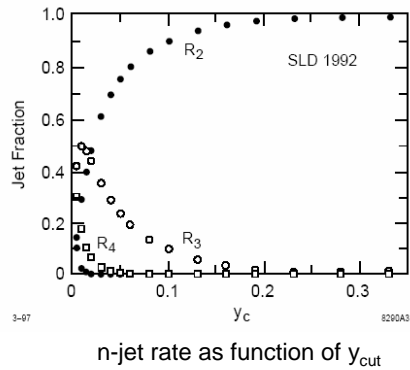
Jet Algorithm

Hadronic particles i and j grouped to a pseudo particle k as long as the invariant mass is smaller than the jet resolution parameter:

$$\frac{m_{ij}^2}{s} < y_{cut}$$

m_{ij} is the invariant mass of i and j .

Remaining pseudo particles are **jets**.



QCD calculations provide a theoretical prediction for $R_3^{\text{theo}}(\alpha_s, y_{cut})$

→ fit $R_3^{\text{theo}}(\alpha_s, y_{cut})$ to the data to determine α_s

→ $\alpha_s(s)$

Similarly other event shape variables (sphericity, thrust,...) can be used to obtain a prediction for α_s

c) α_s from hadronic τ decays

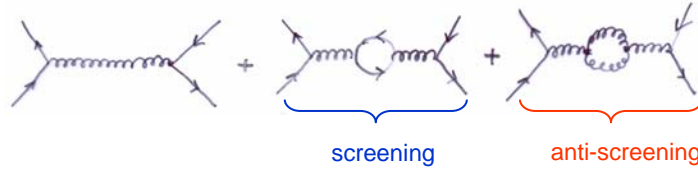
$$R_{had}^{\tau} = \frac{\Gamma(\tau \rightarrow \nu_{\tau} + \text{Hadrons})}{\Gamma(\tau \rightarrow \nu_{\tau} + e\bar{\nu}_e)} \sim f(\alpha_s)$$

→ $\alpha_s(m_{\tau}^2)$

d) α_s from DIS (deep inelastic scattering)

e) Running of α_s

Similar to QED there are propagator corrections to be taken into account



Effective strong coupling $\alpha_s(Q^2)$

$$\alpha_s(Q^2) = \frac{\alpha_s(\mu^2)}{1 + \frac{\alpha_s(\mu^2)}{12\pi} (33 - 2n_f) \log \frac{Q^2}{\mu^2}}$$

n_f = active quark flavors

μ^2 = the renormalization scale

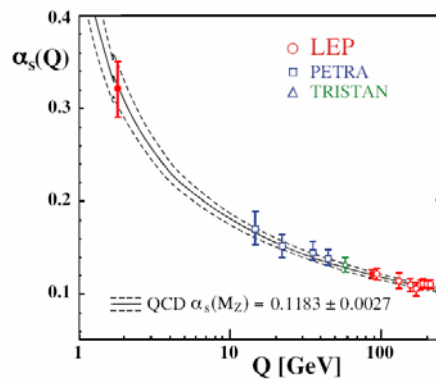
Conventionally renormalization scale is $\mu^2 = M_Z^2$

For $Q^2 \rightarrow \infty$ $\alpha_s \rightarrow 0$:

At large Q^2 quarks are asymptotically free

Running of α_s and asymptotic freedom

$$\alpha_s(Q^2) = \frac{\alpha_s(\mu^2)}{1 + \frac{\alpha_s(\mu^2)}{12\pi} (33 - 2n_f) \log \frac{Q^2}{\mu^2}}$$





The Nobel Prize in Physics 2004



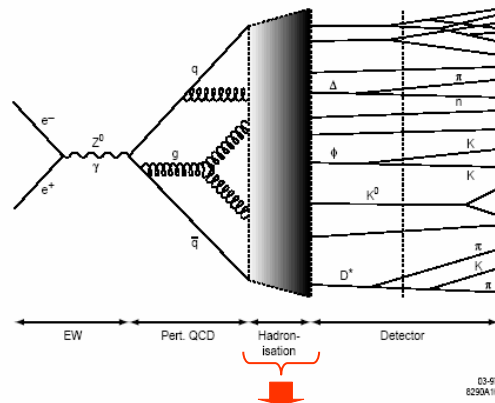
David J. Gross

H. David Politzer

Frank Wilczek

"for the discovery of asymptotic freedom in the theory of the strong interaction"

1.5 Description of hadron production in $e^+ e^-$ annihilation



Described by Monte Carlo programs:

- HERWIG: **Parton shower** (partons are associated to colorless clusters). Clusters with masses larger than M_{Cl} are split.
- JETSET: **String fragmentation**. Color string between colored quarks. Gluons lead to "kinks". Strings are fragmented

2. Structure of the proton

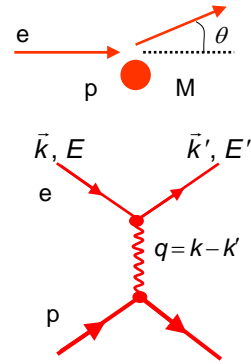
2.1 Elastic electron-proton scattering

General form of diff. cross section

$$\frac{d\sigma}{d\Omega} = \frac{\alpha^2}{4EE' \sin^4 \frac{\theta}{2}} \cdot \frac{E'}{E} \{ \dots \}$$

Rutherford
recoil
non pointlike scattering partners w/ spin

$$-q^2 = 4EE' \sin^2 \frac{\theta}{2}$$



Pointlike target w/o spin
Mott scattering

$$\{ \dots \}_{Mott}^{elastic} = \left(\cos^2 \frac{\theta}{2} \right)$$

Pointlike target w/ spin

$$\{ \dots \}_{e\mu \rightarrow e\mu}^{elastic} = \left(\cos^2 \frac{\theta}{2} - \frac{q^2}{2M^2} \sin^2 \frac{\theta}{2} \right)$$

Extended proton w/ spin

$$\{ \dots \}_{ep \rightarrow ep}^{elastic} = \left(\frac{G_E^2 + \tau G_M^2}{1 + \tau} \cos^2 \frac{\theta}{2} - 2\tau G_M^2 \sin^2 \frac{\theta}{2} \right) \quad \text{mit } \tau = \frac{q^2}{4M^2}$$

Size of the proton

Rosenbluth Plot:

$$\frac{d\sigma}{d\Omega} \Big/ \frac{d\sigma}{d\Omega} \Big|_{Mott} = A(q^2) + B(q^2) \tan^2 \frac{\theta}{2}$$

$$A(q^2) = \frac{G_E^2 - \tau G_M^2}{1 + \tau} \quad \text{mit } \tau = \frac{q^2}{4M^2}$$

$$B(q^2) = -2\tau G_M^2$$



Allows the determination of
electric and magnetic form factors
(Sachs form factors)

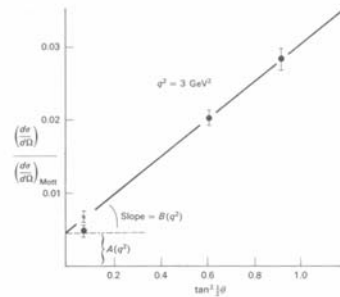


Figure 6.4 The electron-proton scattering cross-section plotted for fixed q^2 and different scattering angles θ (Rosenbluth plot). (After Weber (1967).)

Electric and magnetic form factors can be described by dipole ansatz:

$$G(q^2) = \frac{1}{(1 - \frac{q^2}{0.71 \text{ GeV}^2})^2}$$

Dipole form factor is the Fourier transform of an exponential distribution
 → radius of the charge (magnetic moment) distribution:

$$\langle r^2 \rangle = -6 \frac{dG}{dq^2} \Big|_{q^2=0}$$



$$\langle r_{el}^2 \rangle^{\frac{1}{2}} = \langle r_{mag}^2 \rangle^{\frac{1}{2}} = 0.81 \cdot 10^{-15} \text{ m}$$

Electric and magnetic size of proton and neutron are the same.

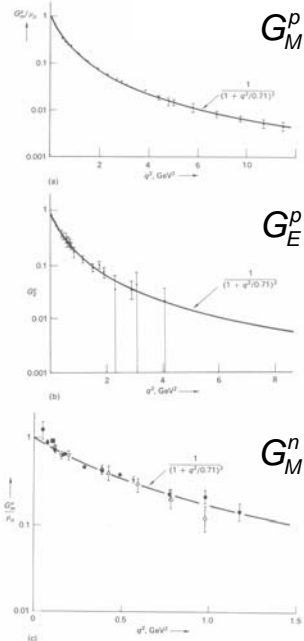
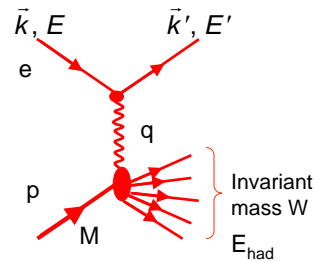


Figure 6.5 Comparison of the magnetic and electric form factors of neutron and proton. They are consistent with the scaling law (6.27). (a) Proton magnetic form factor; (b) proton electric form factor; (c) neutron magnetic form factor. (After Weber (1967).)

2.2 Inelastic ep scattering



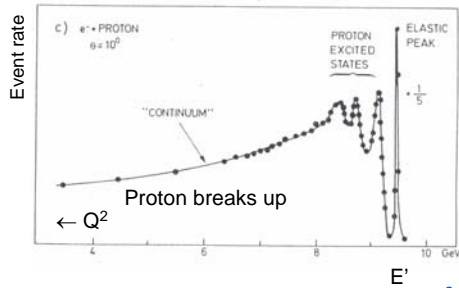
Inelastic scattering: $M \neq W$

2 independent variables:

- $\nu = E - E' = E_{had} - M$
- $q^2 = W^2 - M^2 - 2M\nu = Q^2$

Alternative: Bjorken-Variables

$$x = \frac{Q^2}{2M\nu} \quad \text{and} \quad y = \frac{\nu}{E} \quad \text{Inelasticity}$$



Observation: Large cross section at large Q^2
 From elastic form factor one expects large suppression at large Q^2

Elastic scattering: $W=M$

only one free variable

$$W = M \Rightarrow \frac{Q^2}{2M\nu} = 1$$

a) Differential cross section and structure functions

$$\text{Elastic} \quad \frac{d\sigma}{d\Omega} = \frac{\alpha^2}{4E^2 \sin^4 \frac{\theta}{2}} \cdot \left(\cos^2 \frac{\theta}{2} - \frac{q^2}{2M^2} \sin^2 \frac{\theta}{2} \right)$$

$e\mu \rightarrow e\mu$

$$\text{Inelastic} \quad \frac{d\sigma}{dE'd\Omega} = \frac{\alpha^2}{4E^2 \sin^4 \frac{\theta}{2}} \cdot \left(W_2(\nu, q^2) \cos^2 \frac{\theta}{2} + 2W_1(\nu, q^2) \sin^2 \frac{\theta}{2} \right)$$

$e\mu \rightarrow eX$

$$\frac{d\sigma}{dq^2 d\nu} = \frac{4\pi\alpha^2 E'}{q^4 E} \cdot \left(W_2(\nu, q^2) \cos^2 \frac{\theta}{2} + 2W_1(\nu, q^2) \sin^2 \frac{\theta}{2} \right)$$

With structure functions $W_1(\nu, q^2)$ and $W_2(\nu, q^2)$.

Scattering at point-like objects:

$$2W_1^{point} = \frac{-q^2}{2M^2} \delta(\nu + \frac{q^2}{2M}) \quad W_2^{point} = \delta(\nu + \frac{q^2}{2M})$$

W_1 and W_2 functions of only one variable

b) First measurement of W_2

VOLUME 23, NUMBER 16

PHYSICAL REVIEW LETTERS

20 OCTOBER 1969

OBSERVED BEHAVIOR OF HIGHLY INELASTIC ELECTRON-PROTON SCATTERING

M. Breidenbach, J. I. Friedman, and H. W. Kendall

Department of Physics and Laboratory for Nuclear Science,
Massachusetts Institute of Technology, Cambridge, Massachusetts 02139

and

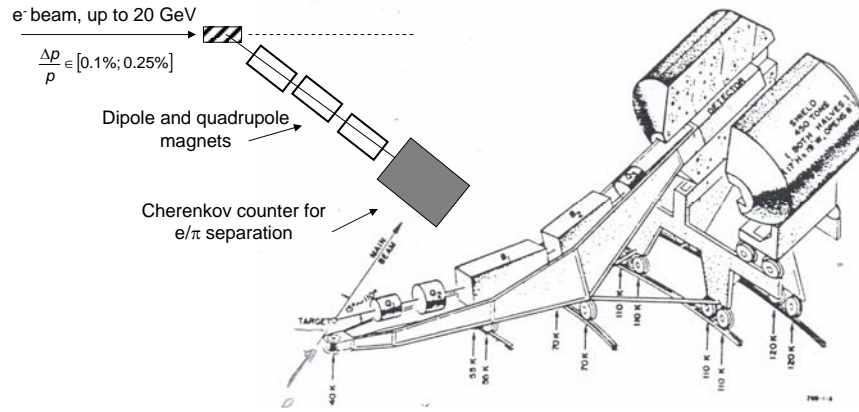
E. D. Bloom, D. H. Coward, H. DeStaabler, J. Drees, L. W. Mo, and R. E. Taylor

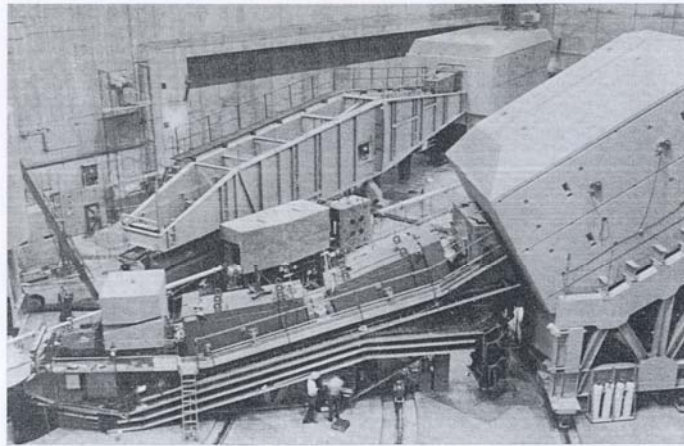
Stanford Linear Accelerator Center, Stanford, California 94305
(Received 22 August 1969)

SLAC & MIT
Experiment

Spectrometer at fixed θ

$$\frac{\Delta p}{p} \sim 0.1\% \quad \Delta\theta \sim 0.7\text{mrad}$$





LARGE MAGNETIC SPECTROMETERS in one of the experimental areas at the SLAC site are used to separate and classify the scattered electrons emerging from the target and to funnel them into a system of detectors. Three spectrometers, each consisting of

a complicated array of magnetic lenses and bending magnets, are installed around a common pivot point in this area; two are visible in this view. The scale of the instruments can be appreciated by noting the two men standing near the "middle-sized" device.

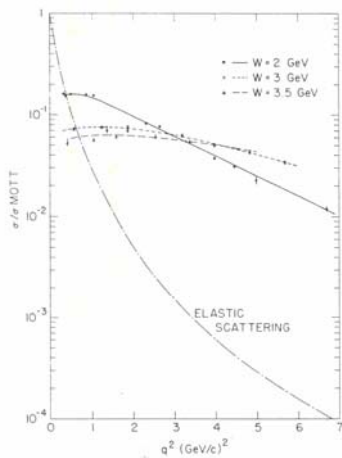
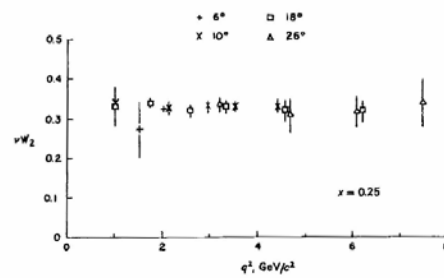


FIG. 1. $(d^2\sigma/d\Omega dE')/\sigma_{\text{MOTT}}$, in GeV^{-1} , vs q^2 for $W = 2, 3,$ and 3.5 GeV. The lines drawn through the data are meant to guide the eye. Also shown is the cross section for elastic $e-p$ scattering divided by σ_{MOTT} , $(d\sigma/d\Omega)/\sigma_{\text{MOTT}}$, calculated for $\theta = 10^\circ$, using the dipole form factor. The relatively slow variation with q^2 of the inelastic cross section compared with the elastic cross section is clearly shown.



Structure function νW_2 does not depend explicitly on Q^2 but depends only on the dimensionless variable x :

$$x = \frac{Q^2}{2M\nu}$$

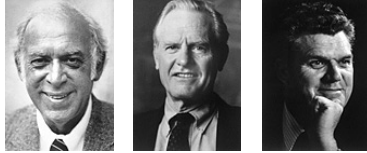
→ **Scale invariance: "scaling"**

Indicates elastic scattering at point-like constituents of the proton: partons

Real sensation in 1970 ...



The Nobel Prize in Physics 1990



Jerome I. Friedman	Henry W. Kendall	Richard E. Taylor
--------------------	------------------	-------------------

"for their pioneering investigations concerning deep inelastic scattering of electrons on protons and bound neutrons, which have been of essential importance for the development of the quark model in particle physics"

c) Structure functions F_1 and F_2

Instead of W_1 and W_2 the structure functions F_1 and F_2 are used today:

$$\left. \begin{aligned} \nu W_2(\nu, Q^2) &\rightarrow F_2(x) = \nu W_2(x = \frac{Q^2}{2M\nu}) \\ MW_1(\nu, Q^2) &\rightarrow F_1(x) = MW_1(x = \frac{Q^2}{2M\nu}) \end{aligned} \right\} \text{dimensionless}$$

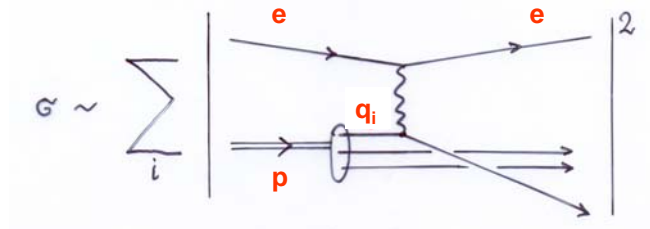
$$\frac{d\sigma}{dq^2 d\nu} = \frac{4\pi\alpha^2}{q^4} \frac{E'}{E} \cdot \left(W_2(\nu, q^2) \cos^2 \frac{\theta}{2} + 2W_1(\nu, q^2) \sin^2 \frac{\theta}{2} \right)$$



$$\frac{d\sigma}{dq^2 d\nu} = \frac{4\pi\alpha^2}{q^4} \frac{E'}{E\nu} \cdot \left(F_2\left(\frac{q^2}{2M\nu}\right) \cos^2 \frac{\theta}{2} + \frac{2\nu}{M} F_1\left(\frac{q^2}{2M\nu}\right) \sin^2 \frac{\theta}{2} \right)$$

$$\frac{d\sigma}{dQ^2 dx} = \frac{4\pi\alpha^2}{Q^4} \frac{E'}{E} \cdot \frac{F_2(x)}{x} \left(\cos^2 \frac{\theta}{2} + \frac{2xF_1(x)}{F_2(x)} \frac{Q^2}{2M^2 x^2} \sin^2 \frac{\theta}{2} \right)$$

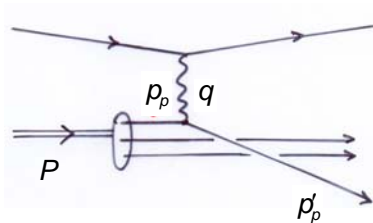
2.3 Parton Model for electron-nucleon scattering: $ep \rightarrow eX$



σ = incoherent sum of all possible parton (quark) contributions

1. Nucleon consists of quasi-free point-like constituents (partons)
2. Lepton scatters elastically on free spin $\frac{1}{2}$ partons
3. Scattered parton interacts strongly with the other constituents (spectators) to form observable hadrons

Infinite momentum frame – Bjorken x



Infinite momentum frame:

- Proton carries infinite momentum
(transverse mom. + mass of quarks can be neglected)

• 4-mom fraction of parton: $p_p = x_p P$

Infinite momentum frame:

$$p_p + q = p'_p$$

$$x_p P + q = p'_p$$

$$p_p^2 + 2x_p Pq + q^2 = p_p'^2$$

$$\Rightarrow q^2 = -2x_p Pq$$

$$= -2x_p Mv$$

Proton rest frame:

$$P = (M, 0)$$

$$q = (v, \vec{q})$$

$$Pq = Mv$$

$$x_p = \frac{-q^2}{2Mv} = \frac{Q^2}{2Mv} \equiv x$$

Consequence of elast. scattering:

$$1 = \frac{-q^2}{2x_p Mv} = \frac{-q^2}{2m_p v}$$

if formally $m_p = x_p M$

Bjorken variable x = momentum fraction of parton